The relationship between molecular weight of bacterial cellulose and the viscosity of its copper (II) ethylenediamine solutions

Huayang Yu · Alexandra Lanot · Ningtao Mao

Abstract There are difficulties in measuring the molecular weight (Mw) of bacterial cellulose (BC) using Gel Permeation Chromatography (GPC) analysis. Additionally, the Mark-Houwink-Sakurada equation cannot be used to predict the Mw of BC as no Mark-Houwink-Sakurada constant specific to BC is available. In this study, a systematic approach is developed to establish the relationship between the Mw of BC and the viscosity of its copper (II) ethylenediamine (CED) solutions. Impurities contained in the raw BC are examined and appropriate purification procedures are designed for their removal before the above two measurements are conducted. The Mw of BC is obtained by measuring the Degree of Polymerization of its corresponding cellulose acetate (CA), derived from degraded BC, using GPC analysis, and

the viscosity of the CED solutions of the BC is measured using a BS/U Tube viscometer. In this paper, the Mark–Houwink–Sakurada constants (K=0.3752 mL/g and α=1.4532) specific for BC are determined to relate the Mw of BC with the intrinsic viscosity of its CED solutions. It is also found that the Mw of BC is proportional to the dynamic viscosity (i.e., $\eta_{BC} = 0.0183 Mw^{1.3069}$) and the flow time (i.e., $t_{BC} = 1.3809 Mw^{1.3062}$) of its CED solutions. These BC-specific relationships can help determine the Mw of BC from the rheological properties of its CED solutions.

Keywords Bacterial cellulose · Flow time · Dynamic viscosity · Intrinsic viscosity · Mark–Houwink–Sakurada constant · Molecular weight

H. Yu (✉) · N. Mao (✉)
School of Design, University of Leeds, Woodhouse Lane, Leeds LS2 9JT, UK
e-mail: h.yu2@leeds.ac.uk

N. Mao
e-mail: n.mao@leeds.ac.uk

A. Lanot
CNAP-Department of Biology, University of York, Wentworth Way, Heslington, York YO10 5DD, UK
e-mail: alexandra.lanot@york.ac.uk

Introduction

BC is chemically analogous to plant cellulose and can be represented by the common formula for cellulose, which is $(C_6H_{10}O_5)_n$ (Tsouko et al. 2015; Gedarawatte et al. 2021; Atykyan et al. 2020; Moghanjougi et al. 2020). BC has a number of distinctive characteristics compared to other cellulose materials, including high DP, high crystallinity, high water-holding capacity, ultrafine network architecture, biocompatibility, biodegradability, non-toxicity, and high mechanical strength (Atykyan et al. 2020; Ghasemi et al. 2020; Brown Jr 1996). The exceptional purity of BC is

characterized by the absence of lignin, hemicellulose, pectin, and other biogenic constituents, and a distinctive three-dimensional (3D) reticulated network structure comprised of cellulose nanofibers (Zhong 2020; Huang et al. 2014; Wang et al. 2019). These attributes render it extensively applicable in diverse sectors, including pharmaceuticals, biomedicine, and the food industry (Blanco et al. 2020; Moniri et al. 2017; Lin et al. 2020). Most of BC is produced by *Acetobacteraceae* family which is well known as acetic acid bacteria (AAB) (Mamlouk and Gullo 2013; Singh et al. 2020). The AAB is a gram-negative obligate aerobe in rod shapes that metabolizes carbon sources (e.g., glucose) into acetic acid and ethanol through oxidative fermentation pathways (Raspor and Goranovič 2008; Singh et al. 2020). It conjugates a glucose monomer (carbon source) with a uridine diphosphate (UDP) group to produce UDP-glucose (Gullo et al. 2018; Singh et al. 2020). Then polymerization between UDP-glucose units occurs under the cellulose synthase complex in the inner membrane of cells (Ross et al. 1991; Singh et al. 2020). The cellulose produced in the AAB cell wall typically crystallizes as cellulose Iα, which has a triclinic unit cell containing one chain, this is a unique feature of BC and differs from the cellulose produced from other sources (Ross et al. 1991; Atalla and Vanderhart 1984; Nishiyama et al. 2002, 2003). For example, the cellulose produced in the plant cells (e.g., vascular plants) is dominated by the crystalline structure of cellulose Iβ (Sugiyama et al. 1991) which has a monoclinic unit cell containing two parallel chains (Atalla and Vanderhart 1984; Nishiyama et al. 2002, 2003). In the cellulose produced from the green algae *Valonia*, both cellulose Iα and Iβ are typically found in the proportions of 65 % and 35 %, respectively, although this proportion can vary in non-algal samples (Sugiyama et al. 1991; Atalla and Vanderhart 1984). Also, cellulose IV, a disordered form of cellulose I (Wada et al. 2004), is found in the cell walls of Oomycetes (Helbert et al. 1997; Bulone et al. 1992).

The ultrafine structure of BC is primarily characterized by robust hydrogen bonding interactions. The hydrogen bonding structures in cellulose Iα and Iβ are similar to each other (Wohlert et al. 2022). However, when these hydrogen bonds exchange with water molecules, their overall impact on the system's energetics becomes relatively minor. Other factors, such as dispersion interactions, play a more critical role

in determining the overall structure (Wohlert et al. 2022). The molecular packing of chains in BC is significantly shaped by steric repulsion and attractive dispersion interactions, which together can account for up to 70 % of the cohesive energy of cellulose (Nishiyama 2018). Consequently, these interactions lead to the formation of densely packed molecular chains within the BC structure (Oberlerchner et al. 2015). This configuration of BC makes it difficult for organic solvent molecules to penetrate its matrix (Oberlerchner et al. 2015), and makes the BC highly resistant to dissolution in organic solvents, which complicates the process of measuring its Mw.

Under certain conditions, such as cold temperatures, BC can crystallize as cellulose II, which is significantly different from either of the two cellulose I structures (Langan et al. 2001; Sawada et al. 2022; Hirai et al. 1997). Despite the limited amount of literature documenting the existence of cellulose II in BC and algal cellulose, the available evidence remains reliable (Sisson 1938; Hirai et al. 1997). It is noticed that the cellulose Iα is metastable and can be converted to cellulose Iβ by annealing in dilute alkali at 260 °C (Sugiyama et al. 1991, 1990). Mercerization of plant cellulose by using sodium hydroxide treatment can transform cellulose I into cellulose II, in which every alternate polymer chain changes direction (Sawada et al. 2022). However, mercerization in BC leads to the folding of polymer chains into a zigzag pattern, forming crystalline anti-parallel domains (Sawada et al. 2022). Tunicate cellulose Iβ is approximately 1.2 % denser than the most crystalline form of cellulose Iα and nearly 2.0 % denser than cellulose II (Langan et al. 2001; Nishiyama et al. 2002, 2003). These density differences are calculated from the unit cell volumes reported in the referenced studies (Langan et al. 2001; Nishiyama et al. 2002, 2003). Further investigation is needed to understand the structure and properties of BC (e.g., Mw) in relation to the cellulose biosynthesis method (Ross et al. 1991; Singh et al. 2020; Brown Jr 1996). For example, the high water-holding capacity is likely attributed to the structure of the BC pellicle, which forms through the somewhat random movements of the bacterium in the culture medium (Brown Jr 1996). Moreover, the Mw, crystallinity, and fibril network structure of BC vary with its production variables, including diverse nutrient solutions, culturing conditions, and purification methods (Choi et al. 2009). The primary impurities

found in raw BC without purification include medium broth and cell biomass, which impact its overall quality (El-Gendi et al. 2022).

The Mw of cellulose constitutes a parameter in the assessment of its characteristics and potential applications. Numerous methodologies are available for the determination of the Mw of cellulose, encompassing techniques such as light scattering, osmotic pressure, end group analysis, ultracentrifugation, and GPC (Oberlerchner et al. 2015; Zhou et al. 2021). While the Mw of cellulose in its DMAc/LiCl solution can be measured directly by using GPC analysis (Potthast et al. 2015), it is found that the DP of cellulose obtained in this way is smaller than the DP of corresponding cellulose derivative measured by using similar GPC analysis. This indicates that cellulose in DMAc/LiCl solution might undergo greater degradation than its corresponding cellulose derivative in DMAc/LiCl solution. It is also found that cellulose from pulps with higher Mw (570 kDa, 498 kDa, and 396 kDa) is hardly dissolved in DMAc/LiCl solution (Potthast et al. 2015). Therefore, the method of measuring the Mw of cellulose in DMAc/LiCl solution by using GPC analysis is not considered in this research. A prevalent approach to determine the Mw of cellulose involves the direct synthesis of cellulose derivatives such as cellulose trinitrate, cellulose tricarbanilate, and CA derived from cellulose (Malešič et al. 2021). Cellulose tricarbanilate can be prepared by reacting cellulose with phenylisocyanate in pyridine at 80 °C (Chang et al. 2021). The resulting cellulose tricarbanilate is soluble in tetrahydrofuran (THF), making it suitable for the determination of Mw using GPC (Chang et al. 2021). CA can be synthesized by reacting cellulose, acetic acid, sulfuric acid, and acetic anhydride at 28 °C for 24 to 48 h (Paiva et al. 2023). The resulting CA is precipitated in excess distilled water at room temperature (Paiva et al. 2023). The Mw of the CA obtained can be determined using GPC after dissolving it in dimethylformamide (DMF) (Paiva et al. 2023). This cellulose derivative synthesis method is associated with certain limitations. There is a possibility for the molecular chains of cellulose to break during the synthesis of CA (Kroon-Batenburg et al. 1996; Klemm et al. 2005). Further reduction of the Mw of the CA might occur when it is dissolved in solvents for GPC analysis. The possible breakage of

molecular chains in both cellulose and its CA during GPC analysis results in a smaller Mw being measured for cellulose compared to its actual Mw (Kroon-Batenburg et al. 1996; Potthast et al. 2015; Maraghechi et al. 2023).

The rheological properties of cellulose solutions are affected by the molecular chain structure and Mw of the cellulose (Gericke et al. 2009). The Mark–Houwink–Sakurada equation for cellulose is used to estimate the Mw of cellulose and predict the rheological behaviour of its CED solutions in the regenerated cellulose fiber spinning (Liu et al. 2016). It establishes the linkage between the Mw of cellulose and the intrinsic viscosity of its CED solutions through appropriate Mark–Houwink–Sakurada constants for various cellulose resources (e.g., wood pulps) (Immergut and Eirich 1953; Maraghechi et al. 2023; Xie et al. 2023; Amini et al. 2023).

Cellulose solutions at low concentrations tend to demonstrate Newtonian characteristics (Maraghechi et al. 2023). Measurement of the intrinsic and dynamic viscosities of such Newtonian cellulose solutions is achieved using a capillary viscometer, such as Ostwald viscometers, Ubbelohde viscometers and BS/U Tube viscometers, which determine the flow time required for the fluid to flow through a narrow capillary tube (Maraghechi et al. 2023). Cellulose solutions are usually prepared by dissolving cellulose in specific solvents such as CED (Wang et al. 2023a), cuprammonium hydroxide (Cuoxam) (Adhikari et al. 2023), cadmium ethylenediamine (Cadoxen) (Wang et al. 2023b), lithium chloride/N, N-dimethylacetamide (LiCl/DMAc) (Bu et al. 2019), lithium hydroxide (LiOH) (Lue et al. 2011), and paraformaldehyde/dimethyl sulfoxide (PF)/DMSO (Eckelt et al. 2009). The Mark–Houwink–Sakurada constants for cellulose in these particular solvents are available in the literature (Wang et al. 2023a; Adhikari et al. 2023; Wang et al. 2023b; Bu et al. 2019; Lue et al. 2011; Eckelt et al. 2009) and Table 1 shows the diverse Mark–Houwink–Sakurada constants pertaining to CED solutions of various types of cellulose (Brandrup et al. 1999).

However, BC is a relatively novel form of cellulose, principally consisting of cellulose I_α and different from the cellulose from plant cells which are principally cellulose I_β, the relationship between the Mw of BC and the dynamic/intrinsic viscosities of its CED solutions remains unclear.

Table 1 Mark–Houwink–Sakurada constants of cellulose from wood (coniferous, deciduous), bamboo, cotton, hemp, straw, jute, flax, reed, sisal in CED solutions (Brandrup et al. 1999)

Solvent	K (mL/g)	α	Molecular weight range (kDa)
	0.00473	0.76	49–970
CED	0.0101	0.9	40–1300
	0.029	0.8	52–150

*1 kDa= 1000 g/mol

Additionally, it has recently found applications in the domain of regenerated cellulose fiber spinning, but there is lack of appropriate Mark–Houwink–Sakurada constants for BC in existing literature for the prediction of its Mw.

The primary objective of this study is to establish the relationship between Mw of BC and dynamic/intrinsic viscosities of its CED solutions, in order to predict the Mw of BC based on its rheological properties. Techniques for examining and removing impurities from raw BC are investigated. The Mw of BC is determined by measuring the Mw of its acetate derivative (i.e., CA) using the GPC analysis. The dynamic and intrinsic viscosities of the CED solutions of the BC are measured by using a BS/U Tube viscometer. The relationships between the Mw of BC and the flow time, as well as the dynamic viscosity of its CED solutions, are established. Mark–Houwink–Sakurada constants for BC are obtained to correlate the Mw of the BC and the intrinsic viscosity of its CED solutions in the Mark–Houwink–Sakurada equation (Kuhn and Kuhn 1948; Sakurada and Taniguchi 1937; Sakurada 2012).

Methodology to obtain the relationship between Mw of BC and viscosities of its CED solutions

This section outlines the methodology employed to obtain Mw of BC and intrinsic/dynamic viscosities of its CED solutions. The flow time of the CED solution of BC is determined using a BS/U Tube viscometer. Relative viscosity (η_r) and specific viscosity (η_{sp}) of

the CED solutions of BC are calculated via Eqs. (1) and (2) (Guimarães et al. 2023).

$$\eta_r = \frac{t_{BC}}{t_0} \tag{1}$$

$$\eta_{sp} = \eta_r - 1 \tag{2}$$

where t_0 and t_{BC} are the flow time of reference CED solution and the CED solutions of BC, respectively, measured in seconds. Intrinsic viscosity (η, mL/g) of the CED solution of BC is determined by Eq. (3), where c is the concentration of BC in its CED solution (g/mL) (Guimarães et al. 2023),

$$\eta = \frac{\sqrt{2\eta_{sp} - ln(\eta_{sp})}}{c} \tag{3}$$

The relationship between Mw (kDa, 1 kDa= 1000 g/mol) of BC and its intrinsic viscosity of its CED solutions is determined via Mark–Houwink–Sakurada equation (see Eq. (4)) (Guimarães et al. 2023; Kuhn and Kuhn 1948; Sakurada 2012; Sakurada and Taniguchi 1937),

$$\eta = KMw^\alpha \tag{4}$$

where η (mL/g) is the intrinsic viscosity obtained from the Eq. (3), the Mark–Houwink–Sakurada constants of both K (mL/g) and α specific for BC are investigated in this research. Dynamic viscosity of CED solutions of BC, η_{BC} (mPa.s) at the concentration of 0.005 g/mL, is defined in the Eq. (5) (Beaulieu et al. 2017),

$$\eta_{BC} = \frac{\eta_{CED}d_{BC}t_{BC}}{d_{CED}t_0} \tag{5}$$

where d_{CED} is the density (1.11 g/mL) of the reference CED solution at the concentration of 1.00 mol/L and d_{BC} is the density (1.11 g/mL) of the CED solution of BC at the concentration of 0.005 g/mL.

In this paper, the concentration of CED solutions of BC is controlled at 0.005 g/mL. The flow time is measured in three replicates using a BS/U Tube viscometer of size B, with the temperature regulated at 25±0.01 °C. The average flow time (t_0) and dynamic viscosity (η_{CED}) of the reference CED solution at the concentration of 1.00 mol/L, are 160.74±0.08 s and

2.14±0.05 mPa.s, respectively, when measured at 25±0.01 °C.

Substituting those constants, $d_{CED} = d_{BC} = 1.11$ g/mL, $t_0 = 160.74±0.08$ s and $\eta_{CED} = 2.14±0.05$ mPa.s into the Eq. (5), the relationship between the dynamic viscosity (η_{BC}) and flow time (t_{BC}) of the CED solutions of BC can be rewritten as Eq. (6).

$$\eta_{BC} = 0.013 t_{BC} \tag{6}$$

The Mw of BC cannot be measured directly due to the insolubility of BC in the solvent (i.e., DMF) used in GPC analysis. Instead, the Mw of CA derived from specific BC of interest is measured in a GPC analyzer. The Degree of Substitution (DS) of the CA, which is defined as the ratio between the absorbance values of C=O stretching to that of O-H stretching (Muzzarelli et al. 1994; Paiva et al. 2023), is characterized by using Fourier Transform Infrared (FTIR) spectroscopy. Then, the molar mass of each unit (Mr) in a CA molecule is calculated using Eq. (7) below (Paiva et al. 2023), and the DP of the CA molecule (or its corresponding BC molecule) is obtained using Eq. (8) (Flory 1953).

$$Mr(kDa) = \frac{159 + 43 \times DS + (3 - DS) \times 1}{1000} \tag{7}$$

$$DP = \frac{Mw \text{ of } CAs}{Mr} \tag{8}$$

Subsequently, the Mw of the corresponding BC is obtained using Eq. (9) below,

$$Mw(kDa) = DP \times 0.162 \tag{9}$$

where 0.162 kDa is the Mr of one unit of cellulose (see Fig. 7).

Experimental

The schematic of the technical route of this study is shown in Fig. 1. It involves the purification of raw BC; degradation of purified BC in $ZnCl_2.4H_2O$ solution for different time durations; measurement of the flow time, dynamic viscosity, and intrinsic viscosity of the degraded BC; synthesis of CA from the degraded BC, and the measurement of the Mw and DP of the CA and BC. Thus, the relationships between the Mw of BC and the flow time, dynamic viscosity and intrinsic viscosity of its CED solutions, including the Mark–Houwink–Sakurada constants specific for BC, are obtained.

The Mw of BC is predicted using the relationships obtained in this study.

Materials and equipment

Four types of BC (A, B, C, and D), produced from an identical bacterial strain of *Komagataeibacter xylinus* under different culturing conditions (e.g., nutrient, temperature, and time duration) (Morrow et al. 2023), were provided by CNAP-Department of Biology, University of York. The extent of differences in
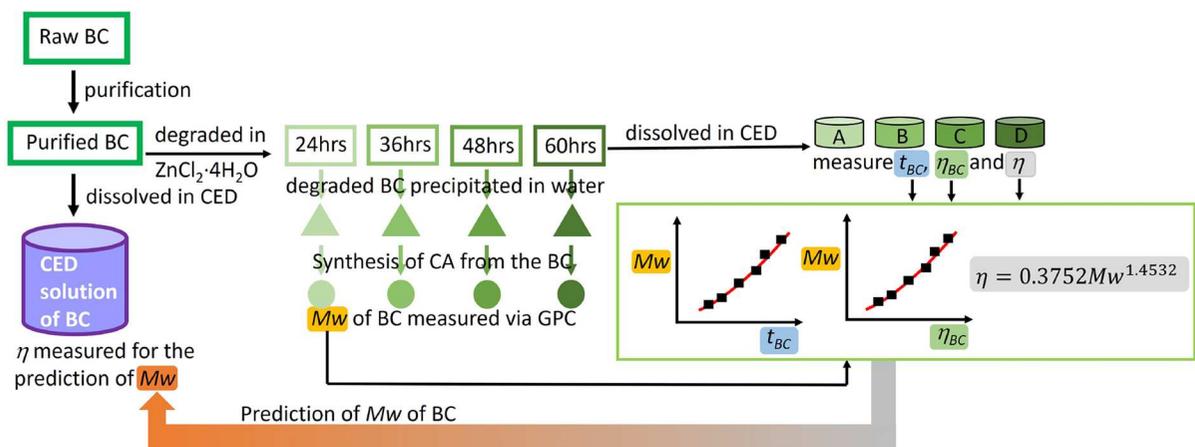

Fig. 1 Schematic of technical route of this study

its Mw is unknown. The morphology and topography of raw BC and processed BC were examined by using Scanning Electron Microscopy (SEM). The elemental composition of the topography of BC materials was analysed employing energy-dispersive X-ray (EDX) analysis in SEM (FEI NanoSEM 450). The results are reported in the section entitled as *Impurities contained in raw BC*.

Chemicals used in the purification, dissolution and analysis of BC are detailed as follows. Vinyl acetate (99 %, stab with 8–12 ppm hydroquinone) was obtained from Alfa Aesar. Dimethyl sulfoxide (DMSO, HPLC grade, 99.9+ %) was purchased from Fisher Scientific. Sodium hydroxide anhydrous pellets (NaOH, reagent grade, ≥98 %), was obtained from Honeywell. Copper (II) ethylenediamine (CED, 1mol/L, VOLUSOL) and 2-propanol (≥98 %, technical), were purchased from VWR Chemicals. DMF (anhydrous, 99.8 %), zinc chloride (anhydrous, powder, ≥99.995 %, trace metals basis), and urea (ACS reagent, 99.0−100.5 %) were obtained from Sigma-Aldrich. Sodium metabisulphite (97+ %, ACS reagent) was purchased from Acros Organics.

Approach 1 for the purification of raw BC: using 20 wt% of NaOH solution

1.0 g of Each type of raw BC was added to 20.0 mL of 20 wt% NaOH solution (mass ratio of raw BC to NaOH is 1:4) and stirred for 20 h at 20 °C (Method 1), 2 h at 60 °C (Method 2) and 2 h at 80 °C (Method 3), respectively. The solution was divided into two equal parts, with one part added to 100.0 mL of ice cold distilled water, and the other part being introduced into 100.0 mL of ice cold propan-2-ol. White precipitate was produced from each solution and collected by centrifuge at 2300 rev/min for 4 min. The white precipitate from the distilled water was dried in an oven at 50 °C for 14 h and in a desiccator for 48 h, and the precipitate from the propan-2-ol was dried in a fume cupboard overnight.

Approach 2 for the purification of raw BC: using urea-bisulphite solution

Urea-bisulphite solution was freshly prepared on the day of use. 125.0 g of Urea and 7.5 g of sodium metabisulphite were dissolved in 80.0 mL of boiling water then the solution was cooled down. 5.0 mL of NaOH solution at the concentration of 5.0 mol/L was added into the above solution and made the volume to 250.0 mL by adding distilled water. The pH of the solution was adjusted to 7.0. 25.0 g of Urea was dissolved in 100.0 mL of distilled water. 20.0 mL of Urea-bisulphite solution was kept at 80 °C for 20 min. 0.2 g of raw BC was added to 20.0 mL of urea-bisulphite solution at 80 °C for 6 h (Method 4). Then the residue was washed by urea solution for three times, and distilled water for six times then dried in an oven at 50 °C for 14 h and in a desiccator for 48 h.

Degradation of purified BC into degraded BC having smaller Mw

It was observed that CA synthesized from purified BC with high Mw was insoluble in DMF, and its solid particles consistently obstructed GPC columns during Mw measurement. Consequently, the purified BC of types A, B, C and D was degraded in a $ZnCl_2.4H_2O$ solution at 60 °C for different periods of time to obtain degraded BC having smaller Mw. The $ZnCl_2.4H_2O$ solution was prepared by dissolving 112.98 g of anhydrous $ZnCl_2$ in 59.77 g of distilled water. 1.22 g of Each type of purified BC was dissolved in 60.28 g of $ZnCl_2.4H_2O$ solution at 60 °C for 24 h, 36 h, 48 h, and 60 h, respectively. The mass ratio of the BC to $ZnCl_2$ was 1:32.3, resulting in 2 wt% of BC-$ZnCl_2$ solution. Then the BC solution was filtered through a stainless-steel mesh with pore size of 20 μm. The BC filtrate was then added to sufficient distilled water to regenerate degraded BC having certain levels of Mw (or DP). The degraded BC was washed with 250.0 mL of distilled water for five times and then dried in an oven at 50 °C for 48 h.

Measurement of dynamic and intrinsic viscosities of the CED solution of BC

The flow time and dynamic viscosity of both the reference CED solution and the CED solution of BC were measured under identical conditions. The CED solutions of BC at the concentration of 0.005 g/mL were prepared by dissolving 0.10 g of purified BC in 20.0 mL of CED solution at 25 °C for certain periods of time. The size of the BC/U Tube viscometer used in the measurement of its intrinsic viscosity depends on the specific concentration of BC in its CED solutions. When the flow time of the solution is greater

than 1000 s, a BS/U Tube viscometer of the size C will be used, with the average flow time of the reference CED solution being 43.11±0.09 s. Triplicate measurements of the flow time of both the reference CED solution and the CED solution of BC were conducted to determine their average flow time.

The intrinsic viscosity and dynamic viscosity were calculated based on the Eqs. (3) and (5), respectively.

Measurement of DP of CA derived from BC using GPC

The Mw and its Dispersity (Đ) (Stepto 2009) of CA derived from specific BC of interest were determined via GPC analysis, and its DP was obtained using the Eqs. (7) and (8) after the measurement of its DS. The Đ is defined as the ratio of the weight-average mass (Mw) to the number-average mass (Mn) (Harrisson 2018), and the DS of the CA was measured using ATR-FTIR spectroscopy to obtain the Mr of each repeating unit in a CA molecule based on the Eqs. (7) (8) and (9) (Paiva et al. 2023).

Synthesis of CA: 1.0 g of each type of degraded BC, 60.0 mL of DMSO, and 15.0 mL of 20 wt% NaOH solution were added to a three-neck round bottom flask, the mixture was stirred at 20°C for 5 min. Then the reaction was under refluxing at 100 °C for 5 min followed by adding 22.0 mL of vinyl acetate and refluxing at 100 °C for further 30 min; then the residue was collected via centrifuging the mixture at 2300 rpm for 4 min. The solution from the mixture was added dropwise to 300.0 mL of ice cold distilled water, yellow precipitate was produced and collected by centrifugation at 2300 rpm for 4 min and dried in an oven at 50 °C overnight.

Measurement of Mw of CA using GPC: Mw of CA derived from specific BC of interest was measured by using a GPC analyzer (model: Agilent 1260 Infinity II) equipped with two PLgel Mixed-C columns plus a guard column and a refractive index detector. DMF containing 0.1 % w/v LiBr was used as the eluent at a flow rate of 1.0 mL/min, and the temperature of the column oven and RI detector were set to 60 °C. 0.021 g of CA was added to 3.0 mL of DMF containing 0.1 % w/v of LiBr and sonicated for 2 h. The solution was filtered using a 0.2 µm syringe filter to remove any insoluble protein and bacterial residues before conducting Mw measurement.

Measurement of DS of CA: DS of CA was determined by obtaining the ratio between the absorbance values of C=O stretching to that of O-H stretching using Attenuated Total Reflection (ATR-Platinum) FTIR spectroscopy (model: Bruker Alpha).

It is anticipated that CA may undergo additional degradation upon sonication-facilitated dissolution in potent solvents such as DMF or THF for the measurement of its Mw using GPC analysis. Thus, the Mw of CA determined through GPC analysis is smaller than that of the original BC used in the analysis. However, the quantification of the reduction of the Mw of CA cannot be ascertained due to the unavailability of the original Mw of BC. It was reported that the average Mw of both cellulose and its acetate derivative exhibited a significant variation of 36.0 % when analyzed using different methods such as GPC with refractive index and GPC with multi-angle laser light scattering (Potthast et al. 2015). Sample preparation, specifically derivatization and dissolution methods, emerged as the two primary influencing factors (Kroon-Batenburg et al. 1996).

Determination of Mw of BC and its relationship with the viscosity of its CED solutions

The DP of BC is assumed to be equivalent to the DP of the corresponding CA; thus the Mw of BC is obtained using Eq. (9) after measuring the DP of CA. The dynamic and intrinsic viscosities of the CED solutions of BC are determined by using the Eqs. (3) and (5). The relationships between the Mw of BC and the flow time, as well as the viscosity of its CED solutions, are thus established for predicting the Mw of BC from its rheological properties.

Results and discussion

Purification of raw BC

Raw BC used in this research contained impurities potentially from culture solutions, including nutrients used for bacterial cultivation, residual bacterial bodies, and proteins generated during the bacterial culturing process. These impurities have the potential to dissolve in several solvents used for the dissolution of BC, such as CED solution, thereby potentially causing inconsistent and erratic measurements of both the

Mw of BC and the viscosity of the CED solutions of BC. Thus, the impurities in the raw BC need to be removed before incorporating the BC into this study.

The four purification methods developed to remove impurities from raw BC involve the use of either NaOH solution (Methods 1–3) or the urea-bisulphite solution (Method 4).

Impurities contained in raw BC

The morphology of the four types of raw BC, A, B, C and D, was examined using SEM analysis. It can be observed that most of the BC nanofibers in the raw BC of types A and B are bonded together by membrane-like polymers (Fig. 2 a and b). There are particles appearing in worm and oval shapes, which might be bacteria, observed in the raw BC of type A and urea-bisulphite solution purified BC of type B (Fig. 2 c and d).

The chemical structure of raw BC was analyzed via FTIR spectroscopy. In the FTIR spectra of raw BC of types A, B, C and D, peaks corresponding to hydroxyl O-H (3400 cm^{-1} and 1387 cm^{-1}), alkane C-H (2920 cm^{-1}), amine N-H (1642 cm^{-1} and 1573 cm^{-1}), and ether C-O (1023 cm^{-1}) groups are observed (Fig. 3), providing evidence of polysaccharides present in the raw BC. Bacterial production is known to yield various microbial polysaccharides containing ether, alcohol, and alkane functional

groups within their chemical structure (Alexander 1965; Qi et al. 2023). Proteins, integral to the structure of living organisms and crucial in enzyme function, are characterized by amine functional groups (Stark 1965; Burnett et al. 2023). The presence of proteins in the culture medium used for the production of raw BC could result in the incorporation of some proteins into the final product. Therefore, the membrane-like polymers covered on the surface of BC nanofibers might be a mixture of polysaccharides, proteins and other impurities. Consequently, it is imperative to eliminate impurities from raw BC prior to its dissolution, facilitating the accurate measurement of the Mw of BC.

Effectiveness of the four purification methods in the removal of impurities from raw BC

In light of the likelihood that the impurities in the raw BC primarily consist of proteins, two solvent solutions, urea-bisulphite solution and 20 wt% NaOH solution, are utilized in the purification Methods 1–4 to eliminate those proteins from the raw BC. The amounts of BC residues obtained after different purification methods are shown in Tables S1–S4 in the Supplementary Information. It is shown that, after treating the raw BC of types A, B, C and D using Method 4, the percentage of BC residues of types of A, B, C and D are 88.3 %, 87.9 %, 95.8 %,

Fig. 2 **a** and **c** Morphology of sheets of raw BC of type A; **b** morphology of sheets of raw BC of type B; **d** morphology of sheets of raw BC of type B after purified by using urea-bisuphite solution
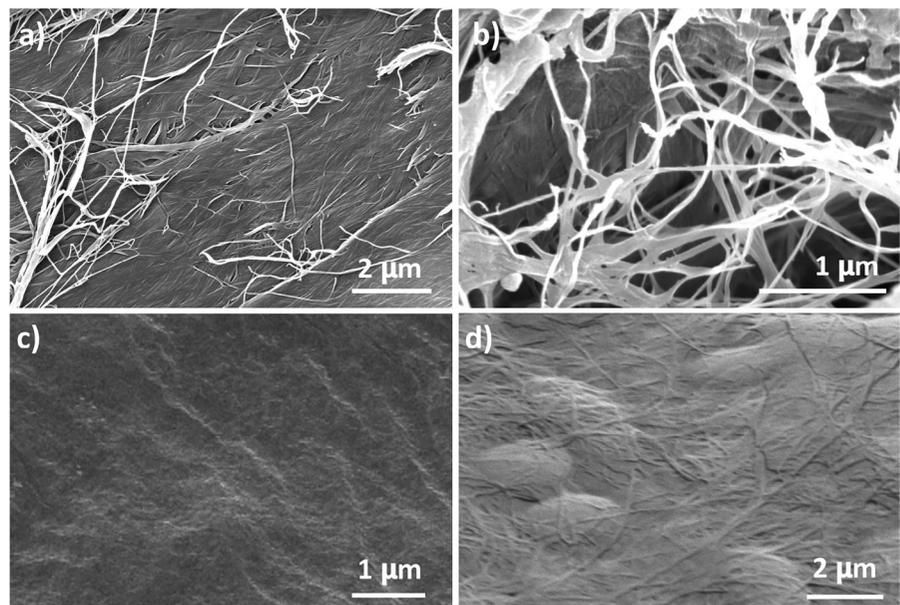
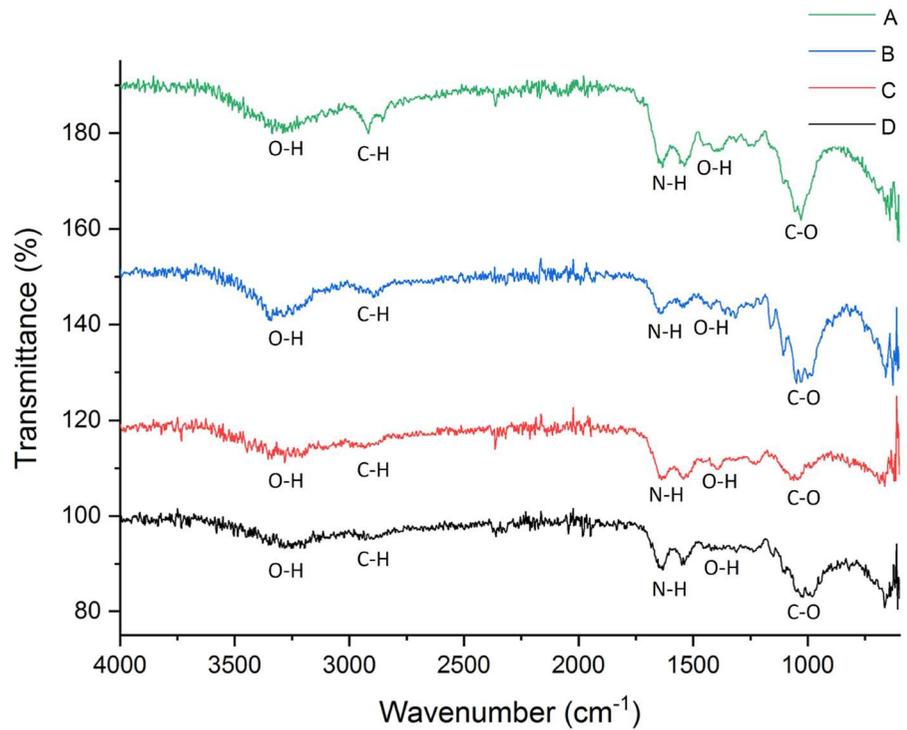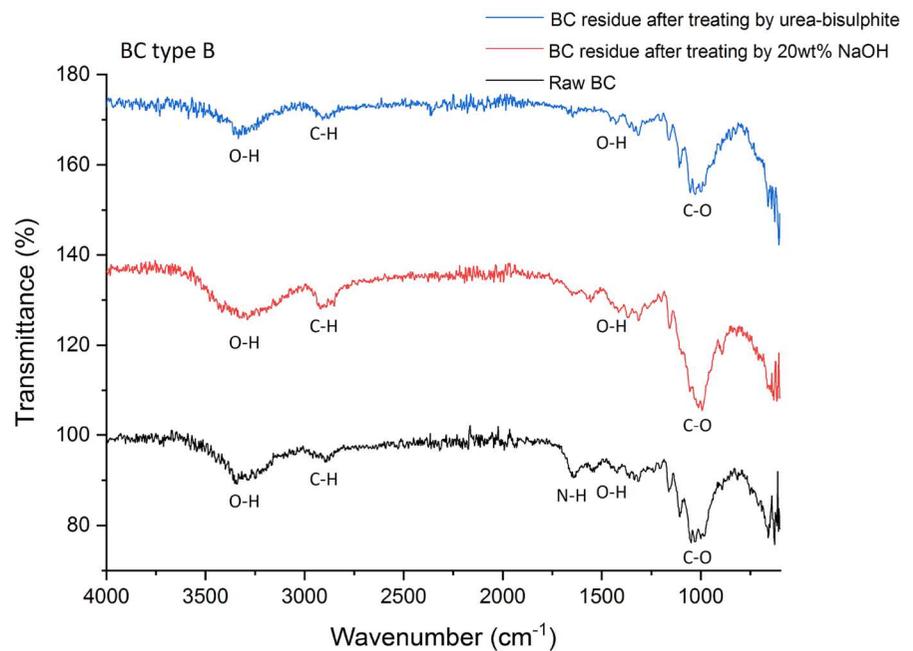**Fig. 3** FTIR spectra of the raw BC of types A, B, C and D

Fig. 4 FTIR spectra of raw BC of type B and the BC after purified with urea-bisulphite solution at 80 °C for 6 h (Method 4) and 20wt% NaOH solution at 20 °C for 20 h (Method 1), respectively

90.0 % respectively, which are greater than those obtained in the Method 1 (72.9 %, 83.5 %, 82.6 %, 81.3 %), Method 2 (68.9 %, 78.4 %, 78.0 %, 77.2 %) and Method 3 (62.2 %, 73.8 %, 72.9 %, 70.7 %) (Tables S1–S4).

In comparison of the FTIR spectra of the BC residues before and after treating with the four methods (Figs. 4, S1–S3), it is observed that the amine N-H (1642 cm^{-1} and 1573 cm^{-1}) peaks for all of the BC purified with Methods 1–3 are significantly reduced (Figs. 4, S1–S3). However, Method 4 only works effectively in removing proteins from raw BC of type B, as evidenced by the disappearance of the amine N-H peak in its FTIR spectra (Fig. 4). Conversely, the amine N-H peaks still appear in the FTIR spectra of BC residues of types A, C and D after treatment using Method 4 (Fig. S1–S3). Therefore, proteins and other impurities on raw BC are dissolved and removed efficiently by Methods 1–3. It is also found that the mass percentage of the residues of the four types of BC after treatment using Method 2 (68.9 %, 78.4 %, 78.0 %, 77.2 %), and Method 3 (62.2 %, 73.8 %, 72.9 %, 70.7 %) are smaller than that using Method 1 (72.9 %, 83.5 %, 82.6 %, 81.3 %). This is believed due to some parts of BC being dissolved in the 20 wt% NaOH solution in Methods 2 and 3.

Further analysis of the compositions of impurities remaining within the raw BC and those dissolved in the 20 wt% NaOH solution was conducted for comprehensive evaluation. After treating the four types of raw BC using Method 1, the resultant solutions were added in ice cold distilled water and ice cold propan-2-ol, respectively. White precipitates were produced

and analyzed via FTIR spectroscopy (Figs. 5, S4–S6). Alcohol O-H (3400 cm^{-1} and 1422 cm^{-1}), amine N-H (1573 cm^{-1}) and alkane C-H (2966 cm^{-1} and 867 cm^{-1}) peaks are observed in the FTIR spectra of the precipitates obtained in water and propan-2-ol from all four types of raw BC (Figs. 5, S4–S6). Additionally, ether C-O (1023 cm^{-1}) peaks are detected in the FTIR spectra of all the white precipitates produced in distilled water (Figs. 5, S4–S6). Therefore, the impurities from raw BC obtained in propan-2-ol and water might be proteins and cellulose (or polysaccharides) with proteins, respectively. It is thus reasonable to conclude that the impurities in the raw BC dissolved in NaOH solutions are mainly proteins (or polysaccharides), while NaOH also dissolves parts of BC. No precipitate was produced from the filtrate obtained using Method 4 when it was added to either distilled water or organic solvents (e.g., acetone, ethanol, propan-2-ol and THF). This indicates that all of the protein impurities might be decomposed into water soluble polypeptides of short chains and amino acids. Therefore, the components of the membrane-like polymers in all types of raw BC are believed to be protein, short chain polypeptides and other impurities.

Fig. 5 FTIR spectra of the white precipitates of raw BC of type B obtained in propan-2-ol and distilled water
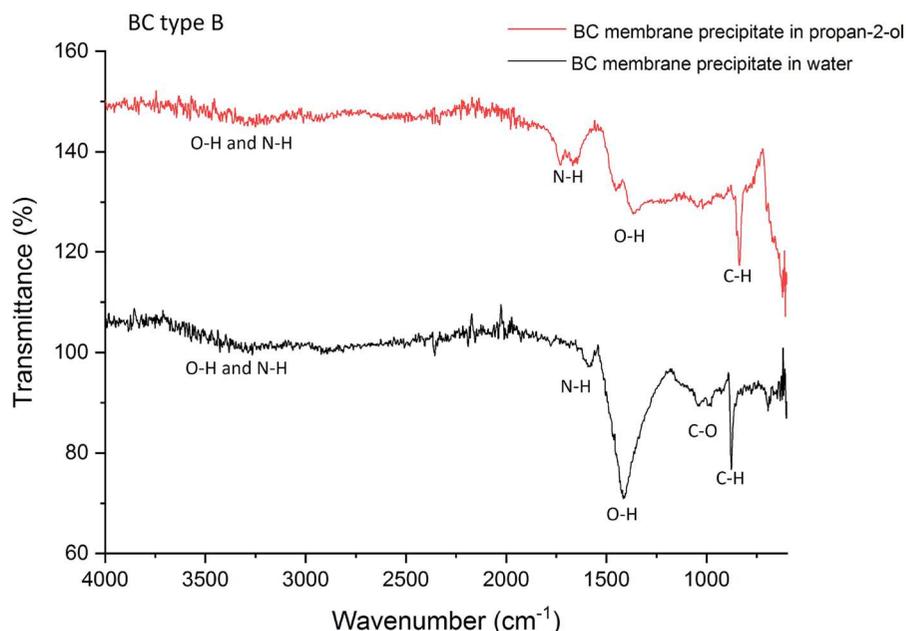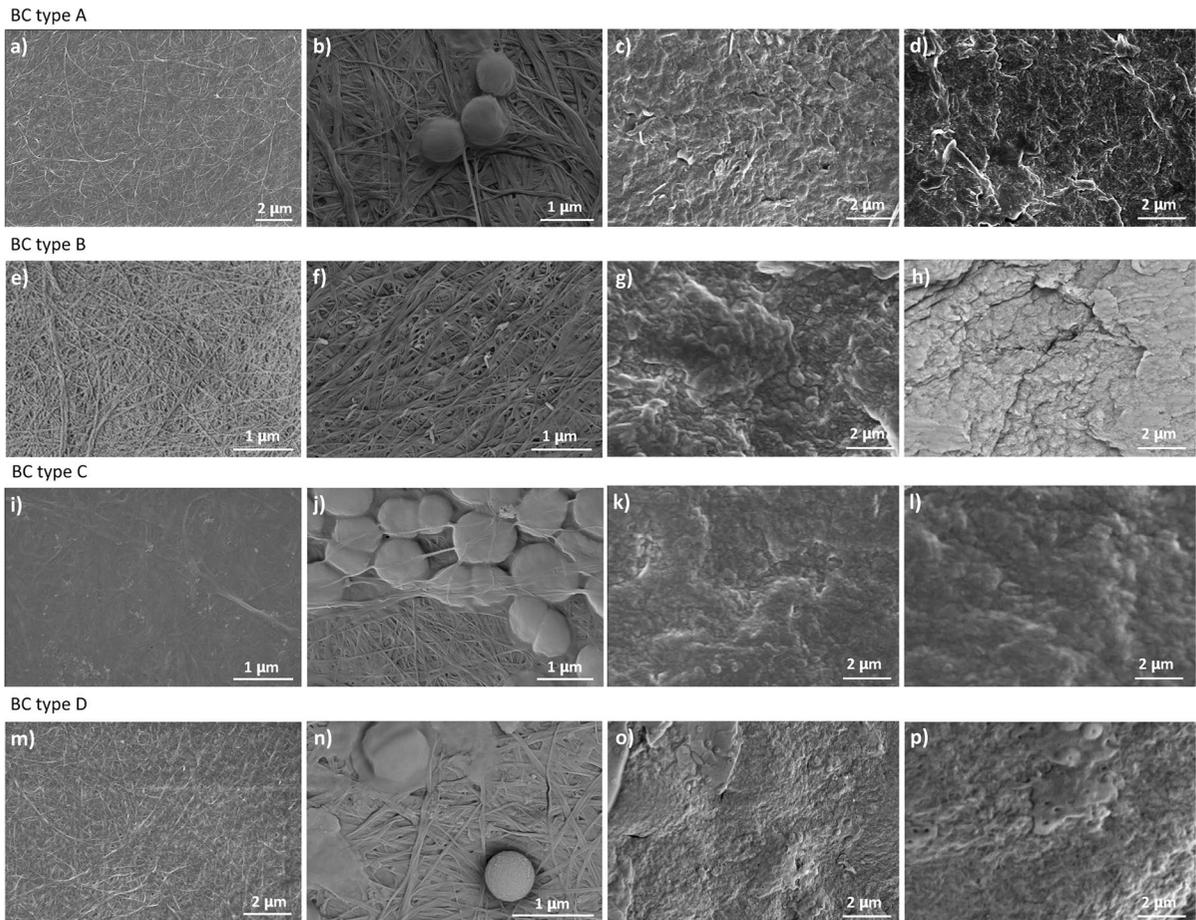
Fig. 6 SEM images of BC of types A, B, C and D, BC treated by Method 1 (**a**, **e**, **i**, **m**), BC treated by Method 4 (**b**, **f**, **j**, **n**), BC treated by Method 2 (c, g, k, o) and BC treated by Method 3 (**d**, **h**, **l**, **p**)

Impurity residues in the BC after different purification processes

SEM analysis of the purified BC residues of types A, B, C, and D using Methods 1–4, are illustrated in Fig. 6. Nanofibers clearly appear on the surface of sheets of BC after all types of raw BC are treated with Methods 1 and 4 (Fig. 6 a, b, e, f, i, j, m, n). Bacteria are not found on the surface of any BC residues after purification using Method 1 (Fig. 6 a, e, i, m). It seems that when the raw BC is treated by Method 1, bacteria contained in all types of BC might undergo degradation into molecules of amino acids and small polypeptides, subsequently removed through a thorough washing procedure with distilled water. The persistence of bacteria within the BC is found in the residue of BC of types A, C, and D after treated with

Method 4 (Fig. 6 b, j, n). The particular BC necessitates more stringent purification treatments to effectively eliminate the bacterial presence. It is found that no bacteria are present in the BC of type B after treated using Method 4 (Fig. 6 f). The small pieces in strip-shape that appear on the surface of BC of type B and that in sphere-shape appear on the surface of BC of type D after treatment using Method 4 (Fig. 6 f, n) are found to be calcium carbonate (aragonite) and silicon, respectively, through EDX analysis (Figs. S7, S8). After treatments with Methods 2 or 3, all of the BC nanofibers are found to still be covered with membrane-like polymers, and no nanofibers or bacteria are shown on the SEM images of the residues of those BC (Fig. 6 c, d, g, h, k, l, o, p). It is thus concluded that, after treatment with Methods 2 and 3, the

Fig. 7 Synthesis of CA via NaOH catalysed transesterification of BC and vinyl acetate at 100°C for 30 min
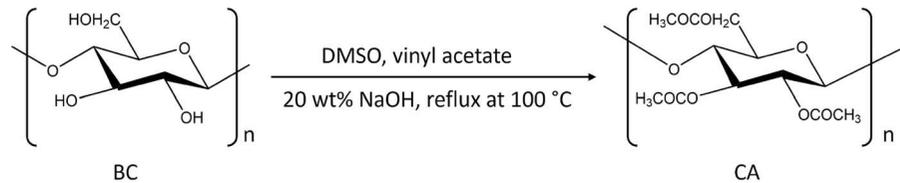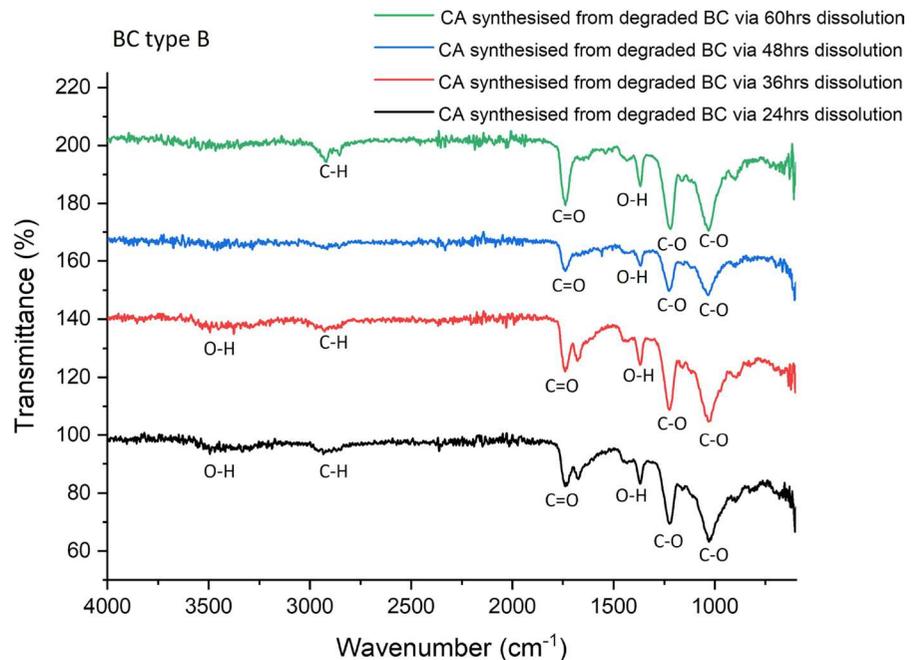

Fig. 8 FTIR spectra of CA synthesised via refluxing degraded BC of type B having different Mw with vinyl acetate for 30 min

impurities, bacteria, and BC nanofibers still remain adhered together.

In a summary, it is suggested that the primary constituent of the membrane-like polymers contained in raw BC is likely to be protein. When subject to a 20 wt% NaOH solution, bacteria, proteins, and certain polysaccharides present in raw BC are effectively dissolved and eliminated. However, it is observed that a small proportion of BC might also be potentially dissolved in the 20 wt% NaOH solution. In contrast, cellulose is hardly dissolved in urea-bisulphite solution used in Method 4, while impurities including bacteria, proteins and certain polysaccharides present on the surface of raw BC might be effectively dissolved and eliminated in this solution. However, Method 4 might not effectively eliminate impurities embedded within the layers of BC, resulting in the retention of some impurities in the purified BC. Notably, the successful removal of protein, bacteria, and other impurities including calcium carbonate and silicon from raw BC is achieved

Table 2 DS of CA synthesized from the degraded BC of types A, B, C and D

CA synthesized from degraded BC via dissolution in $ZnCl_2$ for different periods of time		BC of type A	BC of type B	BC of type C	BC of type D
DS of CA	24 h	2.02	2.06	2.07	2.08
	36 h	2.07	2.04	2.03	2.03
	48 h	2.04	2.11	2.02	2.02
	60 h	2.05	2.08	2.06	2.07

through the application of the purification treatment using Method 1, albeit with a minor loss of cellulose.

CA synthesized from BC and the measurement of its DP

CA was synthesized via NaOH catalysed transesterification of BC and vinyl acetate at 100 °C (Fig. 7) (Cao et al. 2013; French 2017). Transesterification occurred between the hydroxyl groups in the cellulose and vinyl acetate. Progress towards achieving the desired DS in the CA was monitored by using its FTIR spectra (Figs. 8, S9–S11 and Table 2). The presence of C=O (1735 cm^{-1}) and C-O acetate (1225 cm^{-1}) peaks prove that the CA from all BC was synthesized successfully via refluxing with vinyl acetate at 100 °C for 30 min (Figs. 8, S9–S11).

The DS of the CA synthesized from all degraded BC is illustrated in Table 2. Ascertained via FTIR spectroscopy, the ratio between the absorbance of the C=O stretching and the O-H stretching is measured to determine the DS of the CA (Muzzarelli et al. 1994; Paiva et al. 2023). It is revealed in the Table 2 that type of BC and its dissolution time duration have little influence on the DS of the resulting CA. The similarity in its DS values might be attributed to the identical transesterification reaction conditions employed.

The presence of amine peaks in the FTIR spectra of CA (Figs. S9–S11) indicates that proteins (main component of impurities and body of bacteria) might be present in the CA samples. It is noted that amine peaks at 1573 cm^{-1} still present on FTIR spectra of the CA made from the degraded BC of type A dissolution for 24 h and 36 h, CA from the degraded BC of type C dissolution for 24 h, 36 h and 48 h, and the CA from the degraded BC of type D dissolution for 24 h. In contrast, the amine peaks are absent on the FTIR spectra of all CA from the degraded BC of type B, CA from the degraded BC of type A dissolution for 48 h and 60 h, CA from the degraded BC of type C dissolution for 60 h and CA from the degraded BC of type D dissolution for 36 h, 48 h and 60 h (Figs. 8, S9–S11).

Most proteins should be degraded to smaller molecule of amino acids during both the BC dissolution and CA synthesis processes and should be removed by washing with distilled water. Therefore, the application of Method 1 exhibits notable efficacy in eliminating bacteria from raw BC of type B. However, it is found that, in the case of BC of types A, C, and D, there remains a possibility of bacteria persisting even after undergoing purification using Method 1.

Mw of BC measured by using GPC

The CA derived from the degraded BC for its Mw determination should demonstrate a high level of purity, exhibiting minimal susceptibility to the influence of impurities such as proteins. For this reason, the purification treatment of Method 1 was used, although some degree of degradation of BC occurred during this process.

Proteins are generally categorized based on their physical dimensions, often falling within the nanoparticle range, typically ranging from 1 nm to 100 nm in size (Mu et al. 2014). A syringe nonwoven filter with a pore size of 200 nm was used to effectively remove most of the protein nanoparticles exceeding 200 nm in size during the preparation of CA samples for GPC analysis. Any protein nanoparticles smaller than 200 nm that remained insoluble in DMF should not impact the accuracy of measuring the Mw of CA using GPC.

The Mw of CA derived from all degraded BC was evaluated using GPC and is shown in Table S5. The DS of the CA measured by using FTIR spectra is shown in Table 2. The DP of the CA, which is the same as the corresponding BC, is obtained using Eqs. (7) and (8). The Mw of the degraded BC predicted using the DP of CA obtained is shown in Table S6. There are difficulties in consistently measuring the Mw of the purified BC in GPC. Solid particles are frequently observed in DMF solutions when dissolving CA which was synthesized from the BC for GPC analysis. These particles block the guard column of the GPC system and disrupt the measurement process. Thus, we focus on measuring the Mw of degraded BC as well as the rheological properties of its CED solutions in this research. After BC dissolution in ZnCl$_2$ for a period of time, the molecular chains of the degraded BC are notably fractured into smaller molecules of varying chain lengths, leading to elevate Đvalues in the resultant CA (Table S5). For example, the Mw of the CA synthesized from the degraded BC of type B, obtained from the dissolution time durations of 24 h, 36 h, 48 h, and 60 h, are 199.4 kDa, 160.6 kDa, 125.6 kDa, and 92.8 kDa, respectively (Table S5), and corresponding Đ values are 3.05, 3.33, 3.69, and 5.49, respectively (Table S5). It is apparent that their Mw decrease and Đ values increase with the increasing duration of dissolution time. The DS of each CA measured using FTIR is shown in Table 2 and the Mr of each unit of each CA is computed using Eq. (7) (Paiva et al. 2023). The DP of each CA is determined

by dividing the Mw of CA by Mr (as shown in Eq. (8)) which is presented in Table S5, and the Mw of the corresponding degraded BC obtained by using Eq. (9) is shown in Table S6.

The relationship between Mw of BC and dynamic viscosity (and flow time) of its CED solutions

In this paper, the relationships between the Mw of degraded BC and the flow time (t_{BC}), the dynamic viscosity (η_{BC}) of its CED solutions are generated. New Mark–Houwink–Sakurada constants (K=0.3752 mL/g and α=1.4532) are determined for the relationship between the intrinsic viscosity of the CED solution of BC (η) and its Mw. Mw of BC predicted from the flow time of BC dissolved in CED solutions and its Mw determined from the corresponding CA using GPC are presented in Tables S7 and S6, respectively. The relationship between the Mw of the BC, Mw

(kDa), and the flow time of its CED solutions, t_{BC} (seconds), is thus obtained (Fig. 9a) as shown in Eq. (10) below,

$$t_{BC} = 1.3809 Mw^{1.3062} \ (R^2 = 0.98) \tag{10}$$

The Mw of a group of purified BC of types A, B, C, and D is predicted using the above equation as 152.7±2.2 kDa, 149.4±2.2 kDa, 136.0±1.9 kDa, and 134.7±1.9 kDa, respectively (Table 3).

Similarly, the relationship between the Mw of BC (Table S6) and the dynamic viscosity of its CED solutions (Table S8) is obtained in Fig. 9b. It is found that Mw of the BC, Mw, has a nonlinear relationship with the dynamic viscosity of its CED solutions, η_{BC} (mPa.s), as shown in Fig. 9b and Eq. (11) below,

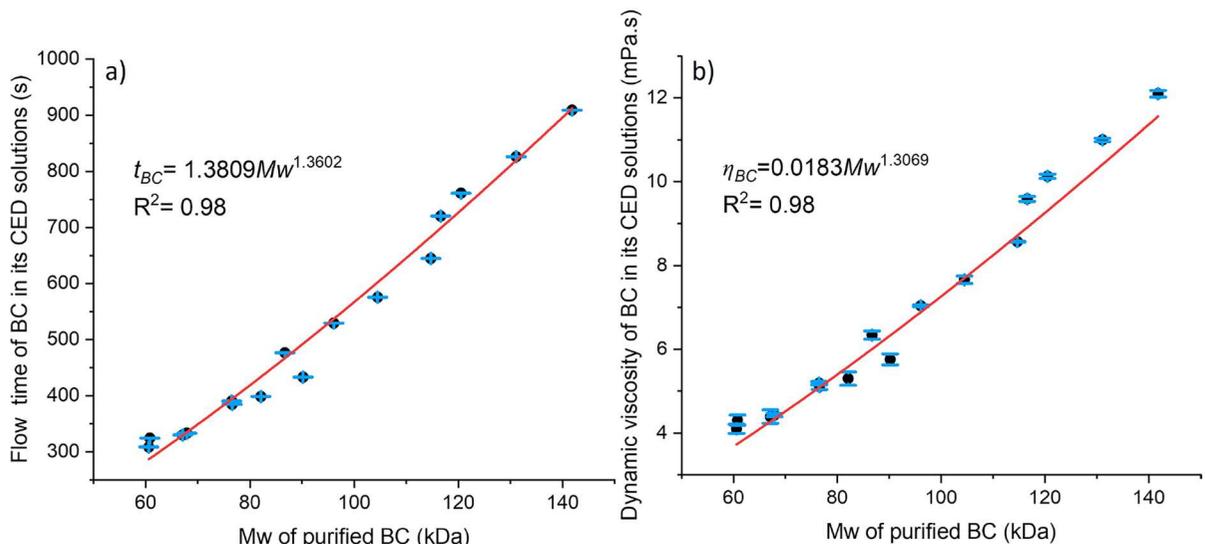$$\eta_{BC} = 0.0183 Mw^{1.3069} \ (R^2 = 0.98) \tag{11}$$

Fig. 9 The relationship between Mw of BC and **a** flow time and **b** dynamic viscosity, of its CED solutions

Table 3 The Mw of a group of purified BC predicted using both the flow time and the dynamic viscosity of its CED solutions

Type of pure BC	A	B	C	D
Flow time of CED solutions of BC (s)	983.3±0.02	955.2±0.2	845.3±0.1	834.4±0.1
Dynamic viscosity of CED solutions of BC (mPa.s)	13.1±0.01	12.7±0.1	11.3±0.03	11.1±0.02
Mw predicted using flow time (kDa)	152.7±2.2	149.4±2.2	136.0±1.9	134.7±1.9
Mw predicted using dynamic viscosity (kDa)	152.8±26.4	149.4±25.8	136.1±23.5	134.7±23.2

*1 kDa= 1000 g/mol

As discussed in the section entitled as *Mw of BC measured by using GPC*, the Mw of purified BC can be predicted here by using the Eqs. (10) and (11). When substituting the dynamic viscosity of the purified BC (Table S8) into Eq. (11), the Mw of BC is predicted as shown in Table 3. The Mw of this group of purified BC of types A, B, C and D predicted using their dynamic viscosity are 152.8±26.4 kDa, 149.4±25.8 kDa, 136.1±23.5 kDa, 134.7±23.2 kDa, respectively, which are close to the Mw of the BC predicted using the flow time (Table 3).

The relationship between Mw of BC and intrinsic viscosity of its CED solutions (i.e., Mark–Houwink–Sakurada equation for BC)

The relationship between the Mw of BC and the intrinsic viscosity (η) of its CED solutions is established using the Mark–Houwink–Sakurada equation (refer to the Eq. 4). New Mark–Houwink–Sakurada constants specified for BC (K= 0.3752 mL/g and α= 1.4532) are produced in this study to correlate the intrinsic viscosity measured (Table S9) and the Mw of BC of types A, B, C, and D obtained by GPC (Table S6). Therefore, the Mark–Houwink–Sakurada equation specifically for BC is as follows,

$$\eta = 0.3752 Mw^{1.4532} \quad (R^2 = 0.98) \quad (12)$$

The comparison between the Mw of purified BC (kDa), predicted using the newly derived Mark–Houwink–Sakurada constants for BC in this study (see the Eq. 12), and that predicted using Mark–Houwink–Sakurada constants for different cellulose obtained from literature, as well as the Mw of BC measured using GPC, are presented in Table 4 and Fig. 10. The supporting data for this comparison are illustrated in Table S10. Both Mw predicted using the newly derived Mark–Houwink–Sakurada constants for purified BC (marked as grey square and labelled as a in the Fig. 10) and the Mw measured by GPC (marked as red dot and labelled as aa in Fig. 10) are quite far away from those predictions using the Mark–Houwink–Sakurada constants for cellulose cited from literature. The Mw of BC, both predicted by using the new Mark–Houwink–Sakurada constants developed in this study and measured via GPC exhibits remarkable proximity (Fig. 10b). Comparatively, the highest Mw of purified BC predicted using literature-based constants is roughly 2.6 times greater than those predicted using the Mark–Houwink–Sakurada constants derived in this study. The Mw predicted by using the new Mark–Houwink–Sakurada constants for BC appears 2–6% smaller (Table 4) than the Mw predicted using both the flow time-Mw and dynamic viscosity-Mw equations (Table 3). It is observed that the Mw of BC measured using GPC (Fig. 9) exhibits
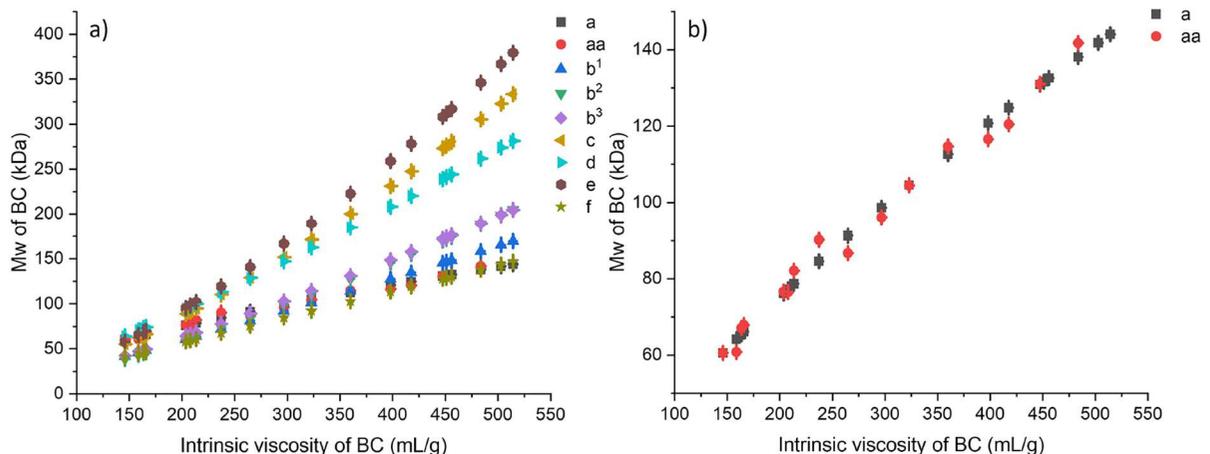

Fig. 10 Mw of BC predicted using the Mark–Houwink–Sakurada equation **a** with the constants both derived in this study (a, grey square), measured by using GPC (aa, red dot) and from existing literature, **b** comparison between the Mw predicted by using the Mark–Houwink–Sakurada equation for BC derived in this study (a, grey) and the Mw of BC measured by using GPC (aa, red dot)

Table 4 Mw of the purified BC of types A, B, C and D predicted using various Mark–Houwink–Sakurada constants K and α (Hiraoki et al. 2015; Brandrup et al. 1999; Kes and Christensen 2013; Ono et al. 2019)

K (mL/g)	α	References	BC type A (kDa)	BC type B (kDa)	BC type C (kDa)	BC type D (kDa)
0.3752	1.4532	This study (a)	144.1	141.9	132.6	131.6
0.0101	0.90	Wood, bamboo, cotton (b[1])	169.7	165.5	148.5	146.7
0.047	0.76	Wood, bamboo, cotton (b[2])	204.6	198.6	174.6	172.1
0.029	0.80	Wood, bamboo, cotton (b[3])	204.6	198.9	176.0	173.6
0.07	0.70	Bleached Softwood (c)	333.3	322.8	280.6	276.4
0.012	0.85	Wood cellulose (d)	281.4	274.1	244.2	241.2
0.094	0.67	Wood cellulose (e)	379.4	366.9	317.0	311.9
0.0035	1.00	Wood cellulose (f)	146.9	143.6	130.2	128.8

*1 kDa= 1000 g/mol

greater fluctuations than the Mw predicted from the new Mark–Houwink–Sakurada constants (Fig. 10b). This discrepancy might be attributed to factors in relation to the dissolution of BC such as the unevenness of BC degradation and variations in the uniformity of different types of BC. Further investigation is necessary to explore these variations. These Mark–Houwink–Sakurada constants for BC are anticipated to have wide uses in the wet fiber spinning process of BC and other BC industries.

Conclusions

This paper presents a systematic approach to obtain the relationship between Mw of BC and the rheological properties of its CED solutions, including the purification of raw BC, characterization of its viscosity, and the measurement of Mw of BC. The research identifies an effective purification method, employing a 20 wt% NaOH solution at 20 °C for 20 h, to treat raw BC effectively and eliminate impurities from it. It establishes a systematic procedure for measuring the Mw of BC by using the GPC analysis method. The relationship between the molecular weight of BC, Mw (kDa), and the dynamic viscosity, η_{BC}, of its CED solutions is established as a form of power function, $\eta_{BC}= 0.0183Mw^{1.3069}$, for the prediction of the Mw of BC

based on the dynamic viscosity of its CED solutions. The relationship between the Mw of BC, Mw (kDa), and the flow time, t_{BC}, of its CED solutions is also proposed, $t_{BC}= 1.3809Mw^{1.3062}$, offering a complementary model for the estimation of Mw of BC. Mark–Houwink–Sakurada constants specific to BC are determined as $K= 0.3752$ mL/g and $\alpha= 1.4532$, (i.e., the Mark–Houwink–Sakurada equation specific for Mw (kDa) of BC is $\eta = 0.3752Mw^{1.4532}$). The resultant relationships and the corresponding methods developed in this study enable the prediction of the Mw of BC based on the viscosities of its CED solutions. These findings are expected to have a wide application in wet spinning of regenerated cellulose fibers from BC and other BC-related industries.

Data availability All data generated or analyzed during this study are included in this published article or its supplementary information files.

Declarations

Conflict of interest The authors declare no Conflict of interest.

Ethical approval and consent to participate Not applicable.

Consent for publication All authors have reviewed and approved the final version of the manuscript, giving explicit consent for its publication.

References

Adhikari J, Dasgupta S, Barui A, Ghosh MSP (2023) Collagen incorporated functionalized bacterial cellulose composite: a macromolecular approach for successful tissue engineering applications. Cellulose 30(14):9079–9111. https://doi.org/10.1007/s10570-023-05407-1

Alexander M (1965) Biodegradation: problems of molecular recalcitrance and microbial fallibility. Appl Microbiol 7:35–80. https://doi.org/10.1016/S0065-2164(08)70383-6

Amini E, Valls C, Yousefi H, MB R (2023) Ionic liquid/ZnO assisted preparation of high barrier cellulose nanocomposite films by in situ ring-opening polymerization of lactide monomers. J Polym Environ 31(6):2576–2594. https://doi.org/10.1007/s10924-022-02740-7

Atalla RH, Vanderhart DL (1984) Native cellulose: a composite of two distinct crystalline forms. Science 223(4633):283–285. https://doi.org/10.1126/science.223.4633.283

Atykyan N, Revin V, Shutova V (2020) Raman and FT-IR spectroscopy investigation the cellulose structural differences from bacteria *Gluconacetobactersucrofermentans* during the different regimes of cultivation on a molasses media. AMB Express 10(1):84. https://doi.org/10.1186/s13568-020-01020-8

Beaulieu L, Logan E, Gering K (2017) An automated system for performing continuous viscosity *versus* temperature measurements of fluids using an ostwald viscometer. Rev Sci Instrum 10(1063/1):4990134

Blanco P, Santoso S, Chou C, Verma V, Wang H, Ismadji S, Cheng K (2020) Current progress on the production, modification, and applications of bacterial cellulose. Crit Rev Biotechnol 40(3):397–414. https://doi.org/10.1080/07388551.2020.1713721

Brandrup J, Immergut EH, Grulke EA, Abe A, Bloch DR (1999) Polymer handbook. Wiley, New York

Brown RM Jr (1996) The biosynthesis of cellulose. JMS-PAC 33(10):1345–1373. https://doi.org/10.1080/10601329608014912

Bu D, Hu X, Yang Z, Yang X, Wei W, Jiang M, Zhou Z, Zaman A (2019) Elucidation of the relationship between intrinsic viscosity and molecular weight of cellulose dissolved in Tetra-*N*-Butyl ammonium hydroxide/dimethyl sulfoxide. Polymers 11(10):1605. https://doi.org/10.3390/polym11101605

Bulone V, Chanzy H, Gay L, Girard V, Fevre M (1992) Characterization of chitin and chitin synthase from the cellulosic cell wall fungus saprolegnia monoïca. Exp Mycol 16(1):8–21. https://doi.org/10.1016/0147-5975(92)90037-R

Burnett AJ, Rodriguez E, Constable S, Lowrance B, WJFish M (2023) Wssl from the Gram-negative bacterial cellulose synthase is an *O*-acetyltransferase that acts on cello-oligomers with several acetyl donor substrates. JBC 299(7):104849. https://doi.org/10.1016/j.jbc.2023.104849

Cao X, Sun S, Peng X, Zhong L, Sun R, Jiang D (2013) Rapid synthesis of cellulose esters by transesterification of cellulose with vinyl esters under the catalysis of NaOH or KOH in DMSO. J Agric Food Chem 61(10):2489–2495. https://doi.org/10.1021/jf3055104

Chang YH, Lin CL, Hsu YH, Lin J (2021) Medium effect on acid degradation of cotton and wood celluloses. Ind Crop Prod 167:113540. https://doi.org/10.1016/j.indcrop.2021.113540

Choi CN, Song HJ, Kim MJ, Chang MH, Kim SJ (2009) Properties of bacterial cellulose produced in a pilot-scale spherical type bubble column bioreactor. Korean J Chem Eng 26:136–140. https://doi.org/10.1007/s11814-009-0021-1

Eckelt J, Eich T, Röder T, Rüf H, Sixta H, Wolf BA (2009) Phase diagram of the ternary system NMMO/water/cellulose. Cellulose 16:373–379. https://doi.org/10.1007/s10570-009-9276-2

El-Gendi H, Taha TH, Ray JB, Saleh AK (2022) Recent advances in bacterial cellulose: a low-cost effective production media, optimization strategies and applications. Cellulose 29(14):7495–7533. https://doi.org/10.1007/s10570-022-04697-1

Flory PJ (1953) Princ Polym Chem. Cornell University Press, New York

French AD (2017) Glucose, not cellobiose, is the repeating unit of cellulose and why that is important. Cellulose 24:4605–4609. https://doi.org/10.1007/s10570-017-1450-3

Gedarawatte ST, Ravensdale JT, Al-Salami H, Dykes G, Coorey R (2021) Antimicrobial efficacy of nisin-loaded bacterial cellulose nanocrystals against selected meat spoilage lactic acid bacteria. Carbohydr Polym 251:117096. https://doi.org/10.1016/j.carbpol.2020.117096

Gericke M, Schlufter K, Liebert T, Heinze T, Budtova T (2009) Rheological properties of cellulose/ionic liquid solutions: from dilute to concentrated states. Biomacromolecules 10(5):1188–1194. https://doi.org/10.1021/bm801430x

Ghasemi S, Bari MR, Pirsa S, Amiri S (2020) Use of bacterial cellulose film modified by polypyrrole/TiO_2-Ag nanocomposite for detecting and measuring the growth of pathogenic bacteria. Carbohydr Polym 232:115801. https://doi.org/10.1016/j.carbpol.2019.115801

Guimarães DT, de Oliveira Barros M, e Silva RA, Silva S, de Almeida J, de Freitas Rosa M, Gonçalves L, Santa Brígida A (2023) Superabsorbent bacterial cellulose film produced from industrial residue of cashew apple juice processing. Int J Biol Macromol. https://doi.org/10.1016/j.ijbiomac.2023.124405

Gullo M, La China S, Falcone PM, Giudici P (2018) Biotechnological production of cellulose by acetic acid bacteria: current state and perspectives. Appl Microbiol Biotechnol 102:6885–6898. https://doi.org/10.1007/s00253-018-9164-5

Harrisson S (2018) The downside of dispersity: Why the standard deviation is a better measure of dispersion in precision polymerization. Polym Chem 9(12):1366–1370. https://doi.org/10.1039/c8py00138c

Helbert W, Sugiyama J, Ishihara M, Yamanaka S (1997) Characterization of native crystalline cellulose in the cell walls of Oomycota. J Biotech 57(1–3):29–37. https://doi.org/10.1016/S0168-1656(97)00084-9

Hirai A, Tsuji M, Horii F (1997) Communication: culture conditions producing structure entities composed of cellulose i and ii in bacterial cellulose. Cellulose 4:239–245. https://doi.org/10.1023/A:1018439907396

Hiraoki R, Ono Y, Saito T, Isogai A (2015) Molecular mass and molecular-mass distribution of TEMPO-oxidized celluloses and TEMPO-oxidized cellulose nanofibrils. Biomacromolecules 16(2):675–681. https://doi.org/10.1021/bm501857c

Huang Y, Zhu C, Yang J, Nie Y, Chen C, Sun D (2014) Recent advances in bacterial cellulose. Cellulose 21:1–30. https://doi.org/10.1007/s10570-013-0088-z

Immergut EH, Eirich FR (1953) Intrinsic viscosities and molecular weights of cellulose and cellulose derivatives. Ind Eng Chem 45(11):2500–2511. https://doi.org/10.1021/ie50527a039

Kes M, Christensen BE (2013) A re-investigation of the Mark-Houwink-Sakurada parameters for cellulose in cuen: a study based on size-exclusion chromatography combined with multi-angle light scattering and viscometry. J Chromatogr A 1281:32–37. https://doi.org/10.1016/j.chroma.2013.01.038

Klemm D, Heublein B, Fink HP, Bohn A (2005) Cellulose: fascinating biopolymer and sustainable raw material. Angew Chem Int Ed 44(22):3358–3393. https://doi.org/10.1002/anie.200460587

Kroon-Batenburg L, Bouma B, Kroon J (1996) Stability of cellulose structures studied by MD simulations. Could mercerized cellulose II be parallel? Macromolecules 29(17):5695–5699. https://doi.org/10.1021/ma9518058

Kuhn W, Kuhn H (1948) Rigidity of chain molecules and its determination from viscosity and flow birefringence in dilute solutions. J Colloid Sci 3(1):11–32. https://doi.org/10.1016/0095-8522(48)90003-8

Langan P, Nishiyama Y, Chanzy H (2001) X-ray structure of mercerized cellulose ii at 1 å resolution. Biol Macromol 2(2):410–416. https://doi.org/10.1021/bm005612q

Lin D, Liu Z, Shen R, Chen S, Yang X (2020) Bacterial cellulose in food industry: current research and future prospects. Int J Biol Macromol 158:1007–1019. https://doi.org/10.1016/j.ijbiomac.2020.04.230

Liu J, Zhang J, Zhang B, Zhang X, Xu L, Zhang J, He J, Liu C (2016) Determination of intrinsic viscosity-molecular weight relationship for cellulose in BmimAc/DMSO solutions. Cellulose 23:2341–2348. https://doi.org/10.1007/s10570-016-0967-1

Lue A, Liu Y, Zhang L, Potthas A (2011) Light scattering study on the dynamic behaviour of cellulose inclusion complex in LiOH/urea aqueous solution. Polymer 52(17):3857–3864. https://doi.org/10.1016/j.polymer.2011.06.034

Malešič J, Kraševec I, Kralj Cigić I (2021) Determination of cellulose degree of polymerization in historical papers with high lignin content. Polymers 13(12):1990. https://doi.org/10.3390/polym13121990

Mamlouk D, Gullo M (2013) Acetic acid bacteria: physiology and carbon sources oxidation. Indian J Microbiol 53:377–384. https://doi.org/10.1007/s12088-013-0414-z

Maraghechi S, Dupont AL, Cardinaels R, Paris-Lacombe S, Hoefnagels P, Suiker S, Bosco E (2023) Assessing rheometry for measuring the viscosity-average degree of polymerisation of cellulose in paper degradation studies. Herit Sci 11(1):15. https://doi.org/10.1186/s40494-022-00855-7

Moghanjougi ZM, Bari MR, Khaledabad MA, Almasi H, Amiri S (2020) Bio-preservation of white brined cheese (feta) by using probiotic bacteria immobilized in bacterial cellulose: optimization by response surface method and characterization. LWT 117:108603. https://doi.org/10.1016/j.lwt.2019.108603

Moniri M, Boroumand Moghaddam A, Azizi S, Rahim R, Ariff A, Saad W, Navaderi M, Mohamad R (2017) Production and status of bacterial cellulose in biomedical engineering. Nanomaterials 7(9):257. https://doi.org/10.3390/nano7090257

Morrow R, Ribul M, Eastmond H, Lanot A, Baurley S (2023) Bio-producing bacterial cellulose filaments through co-designing with biological characteristics. Materials 16(14):4893. https://doi.org/10.3390/ma16144893

Mu Q, Jiang G, Chen L, Zhou H, Fourches D, Tropsha A, Yan B (2014) Chemical basis of interactions between engineered nanoparticles and biological systems. Chem Rev 114(15):7740–7781. https://doi.org/10.1021/cr400295a

Muzzarelli RA, Ilari P, Petrarulo M (1994) Solubility and structure of N-carboxymethylchitosan. Int J Biol Macromol 16(4):177–180. https://doi.org/10.1016/0141-8130(94)90048-5

Nishiyama Y (2018) Molecular interactions in nanocellulose assembly. Philos Trans R Soc A 376(2112):20170047. https://doi.org/10.1098/rsta.2017.0047

Nishiyama Y, Langan P, Chanzy H (2002) Crystal structure and hydrogen-bonding system in cellulose iβ from synchrotron x-ray and neutron fiber diffraction. J Am Chem Soc 124(31):9074–9082. https://doi.org/10.1021/ja0257319

Nishiyama Y, Sugiyama J, Chanzy H, Langan P (2003) Crystal structure and hydrogen bonding system in cellulose iα from synchrotron x-ray and neutron fiber diffraction. J Am Chem Soc 125(47):14300–14306. https://doi.org/10.1021/ja037055w

Oberlerchner JT, Rosenau T, Potthast A (2015) Overview of methods for the direct molar mass determination of cellulose. Molecules 20(6):10313–10341. https://doi.org/10.3390/molecules200610313

Ono Y, Funahashi R, Isogai A (2019) Size-exclusion chromatography with on-line viscometry of various celluloses with branched and linear structures. Cellulose 26:1409–1415. https://doi.org/10.1007/s10570-018-2154-z

Paiva MT, da Silva JB, Brisola J, de Carvalho G, Mali S (2023) Cellulose acetate from lignocellulosic residues: an eco-friendly approach based on a hydrothermal process. Int J Biol Macromol 243:125237. https://doi.org/10.1016/j.ijbiomac.2023.125237

Potthast A, Radosta S, Saake B, Lebioda S, Heinze T, Henniges U, Isogai A, Koschella A, Kosma P, Rosenau T, Schiehser S, Sixta H, Strlič M, Strobin G, Vorwerg W, Wetzel H (2015) Comparison testing of methods for gel permeation chromatography of cellulose: coming closer to a standard protocol. Cellulose 22:1591–1613. https://doi.org/10.1007/s10570-015-0586-2

Qi J, Zhou Q, Huang D, Yu Z, Meng F (2023) Construction of synthetic anti-fouling consortia: fouling control effects and polysaccharide degradation mechanisms. Microb Cell Fact 22(1):230. https://doi.org/10.1186/s12934-023-02235-7

Raspor P, Goranovič D (2008) Biotechnological applications of acetic acid bacteria. Crit Rev Biotechnol 28(2):101–124. https://doi.org/10.1080/07388550802046749

Ross P, Mayer R, Benziman M (1991) Cellulose biosynthesis and function in bacteria. Microbiol Rev 55(1):35–58. https://doi.org/10.1128/mr.55.1.35-58.1991

Sakurada I (2012) Shape of threadlike molecules in solution, and relationship between solution viscosity and molecular weight. Polym J 44(1):5–10. https://doi.org/10.1038/pj.2011.121

Sakurada I, Taniguchi M (1937) Über die diffusion von heterodispersen stoffen. Z Phys Chem 179(1):227–234. https://doi.org/10.1515/zpch-1937-17921

Sawada D, Nishiyama Y, Shah R, Forsyth VT, Mossou E, Oneill HM, Wada M, Langan P (2022) Untangling the threads of cellulose mercerization. Nat Commun 13(1):6189. https://doi.org/10.1038/s41467-022-33812-w

Singh A, Walker KT, Ledesma-Amaro R, Ellis T (2020) Engineering bacterial cellulose by synthetic biology. Int J Mol Sci 21(23):9185. https://doi.org/10.3390/ijms21239185

Sisson WA (1938) The existence of mercerized cellulose and its orientation in halicystis as indicated by x-ray diffraction analysis. Science 87(2259):350–350. https://doi.org/10.1126/science.87.2259.350.a

Stark GR (1965) Reactions of cyanate with functional groups of proteins III. Reactions with amino and carboxyl groups. Biochemistry 4(6):1030–1036. https://doi.org/10.1021/bi00882a008

Stepto RF (2009) Dispersity in polymer science (iupac recommendations 2009). Pure Appl Chem 81(2):351–353. https://doi.org/10.1351/PAC-REC-08-05-02

Sugiyama J, Okano T, Yamamoto H, Horii F (1990) Transformation of Valonia cellulose crystals by an alkaline hydrothermal treatment. Macromolecules 23(12):3196–3198. https://doi.org/10.1021/ma00214a029

Sugiyama J, Vuong R, Chanzy H (1991) Electron diffraction study on the two crystalline phases occurring in native cellulose from an algal cell wall. Macromolecules 24(14):4168–4175. https://doi.org/10.1021/ma00014a033

Tsouko E, Kourmentza C, Ladakis D, Kopsahelis N, Mandala I, Papanikolaou S, Paloukis F, Alves V, Koutinas A (2015) Bacterial cellulose production from industrial waste and by-product streams. Int J Mol Sci 16(7):14832–14849. https://doi.org/10.3390/ijms160714832

Wada M, Heux L, Sugiyama J (2004) Polymorphism of cellulose I family: reinvestigation of cellulose IV$_I$. Biomacromolecules 5(4):1385–1391. https://doi.org/10.1021/bm0345357

Wang J, Tavakoli J, Tang Y (2019) Bacterial cellulose production, properties and applications with different culture methods-a review. Carbohydr Polym 219:63–76. https://doi.org/10.1016/j.carbpol.2019.05.008

Wang Q, Zhao H, Zhao L, Huang M, Tian D, Deng S, Hu J, Zhang X, Shen F (2023) Fabrication of regenerated cellulose fibers using phosphoric acid with hydrogen peroxide treated wheat straw in a DMAc/LiCl solvent system. Cellulose 30(10):6187–6201. https://doi.org/10.1007/s10570-023-05263-z

Wang Z, Jiang Y, Mao L, Mao S, Deng M, Liang X (2023) Pilot-scale preparation of cellulose/carboxymethylcellulose composite fiber for methylene blue adsorption. Cellulose 30(6):3611–3623. https://doi.org/10.1007/s10570-023-05109-8

Wohlert M, Benselfelt T, Wågberg L, Furó I, Berglund LA, Wohlert J (2022) Cellulose and the role of hydrogen bonds: not in charge of everything. Cellulose 29:1–23. https://doi.org/10.1007/s10570-021-04325-4

Xie H, Fan Y, Lu D, Yang H, Zou Y, Wang X, Ji X, Si C (2023) Preparation of zwitterionic cellulose nanofibers with betaine-oxalic acid DES and its multiple performance characteristics. Cellulose 30(17):10953–10969. https://doi.org/10.1007/s10570-023-05566-1

Zhong C (2020) Industrial-scale production and applications of bacterial cellulose. Front Bioeng Biotechnol 8:605374. https://doi.org/10.3389/fbioe.2020.605374

Zhou Y, Zhang X, Zhang J, Cheng Y, Wu J, Yu J, Zhang J (2021) Molecular weight characterization of cellulose using ionic liquids. Polym Test 93:106985. https://doi.org/10.1016/j.polymertesting.2020.106985